

Article

CO₂ Capture by Alkaline Solution for Carbonate Production: A Comparison between a Packed Column and a Membrane Contactor

Israel Ruiz Salmón *, Nicolas Cambier and Patricia Luis 

Materials & Process Engineering (iMMC-IMAP), Université Catholique de Louvain, Place Sainte Barbe 2, 1348 Louvain-la-Neuve, Belgium; nicolas.cambier@gmail.com (N.C.); patricia.luis@uclouvain.be (P.L.)

* Correspondence: israel.ruizsalmon@uclouvain.be

Received: 25 May 2018; Accepted: 15 June 2018; Published: 19 June 2018



Abstract: A comparison between a traditional packed column and a novel membrane contactor used for CO₂ absorption with carbonate production is addressed in this paper. Membrane technology is generally characterized by a lower energy consumption, it offers an independent control of gas and liquid streams, a known interfacial area and avoids solvent dragging. Those advantages make it a potential substitute of conventional absorption towers. The effect of the concentration and the flow rates of both the flue gas (10–15% of CO₂) and the alkaline sorbent (NaOH, NaOH/Na₂CO₃) on the variation of the species present in the system, the mass transfer coefficient, and the CO₂ removal efficiency was evaluated. Under the studied operation conditions, the membrane contactor showed very competitive results with the conventional absorption column, even though the highest mass transfer coefficient was found in the latter technology. In addition, the membrane contactor offers an intensification factor higher than five due to its compactness and modular character.

Keywords: CO₂ capture; membrane contactor; packed column; intensification

1. Introduction

The concentration of carbon dioxide (CO₂) in the atmosphere has increased significantly from about 280 ppm in 1750 (pre-industrial era) to 367 ppm in 1999 [1] and has recently reached the value of 408 ppm [2]. Consequently, global temperature has increased (17 of the 18 warmest years on record have occurred since 2001), the 40% arctic extent has decreased from 1980, and global average sea level has risen almost 2 centimeters over the past 100 years [2].

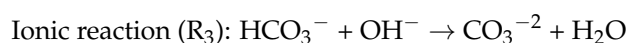
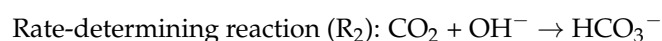
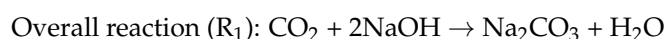
Industry accounts for one-third of all the energy used globally, for almost 40% of worldwide CO₂ emissions, and around 30% of CO₂ released to the atmosphere comes from fossil fuel power plants [3]. However, although CO₂ capture is a global issue, there is no simple solution that can be applied on a global scale.

The most extended capture method is absorption using amines (e.g., monoethylamine or MEA). Nevertheless, there are still some gaps in this technology. Apart from the solvent loss during the process [4] and the large amount of heat that is required to regenerate the solvent [5], critical operating limitations exist, such as emulsions, foaming or flooding [6], and amines, which are very toxic compounds. In addition, the current technology is destined to CO₂ sequestration for further transport by pipeline or ship and injection into a storage site, normally an underground geological formation or the ocean. Alternative technologies are thus a key issue in the development of processes for CO₂ capture and/or reutilization, such as absorption using novel solvents (e.g., ionic liquids), calcium looping, adsorption, and membrane technology [7].

Ionic liquids (organic salts with a melting point below 100 °C) have negligible vapor pressure and are considered in separation and reaction, but their high viscosity and price in comparison with

conventional absorbers do not show any advantages from an economic point of view [8,9]. Calcium looping technology is based on the reaction of CO₂ and calcium oxide (CaO) to obtain calcium carbonate, which is calcined to produce pure CO₂ for sequestration [10]. Although the low price, abundant natural source of CaO and the possibilities of an integrated system power plant-cement plant-CO₂ capture [11], this technology has several challenges: the fast decay in CO₂ carrying capacity (i.e., the level of conversion) over long cycles, the sorbent reactivity decay due to competing reactions, ash fouling or loss of materials, and its reactivation with thermal or chemical treatments [7]. In CO₂ adsorption, the gas diffuses into adsorbent pores of a solid that should have high adsorption capacity and selectivity for CO₂, chemical stability to impurities, low cost, etc. [12,13]. Activated carbon and zeolite-based sorbents are the most common adsorbents because of the low regeneration energy, cheap cost, and fast adsorption kinetics, but they are strongly influenced by temperature, pressure, and the presence of moisture [7]. Metal organic frameworks have more adsorption capacity than zeolites and the water adsorption affect less but the study of higher selectivities and capacities must occur [14].

Regarding membrane technology, research focused on CO₂ capture started around 1990 and since then, great advances have occurred: higher mass transfer coefficients, new materials for membrane synthesis, integration of membrane-based technology, etc. Nowadays, there are two main approaches for CO₂ capture with membranes [15]. First, membranes can be used as selective barriers that determine which compound permeates faster. Gas permeation (the membrane has a dense structure) and supported liquid membranes (there is liquid inside the membrane pores that is responsible for the separation) are the most common technologies applied in this sense [7]. Here, permeability and selectivity are the principal properties. Research in membrane performance, materials and additives has been done with successful results, from a technical point of view [16–18], but their economic viability is not demonstrated [19]. The second main approach in membrane technology for CO₂ capture is the use of membrane contactors as a non-selective barrier, which is considered in this work due to its well-known advantages, such as flexibility on the operation, controlled and known interfacial area, easy and proportional scale-up, low energy needs, and no solvent drop dragging because of the precise separation of both phases [7]. The membrane role is to increase the surface for the mass transfer exchange between both phases; i.e., the feed gas and the absorption liquid—by the action of a driving force [20] and the principal parameter to evaluate the process is the overall mass transfer coefficient. Several absorption liquids are used in this field but a general concern is the regeneration of the absorption liquid or the valorization of CO₂. Large emissions of CO₂ into the atmosphere are a concern that could become an opportunity for the industry if a valuable compound can be produced at minimum cost. The approach of our work tries to recover CO₂ as sodium carbonate (Na₂CO₃), following previous works that showed the technical viability of the carbonate production as pure crystals [21–24], independently of the amount of impurities on the NaOH-containing streams. This is particularly interesting in pulp and paper, water treatment, and certain chemical sectors where NaOH can be substituted for sodium carbonate (Na₂CO₃) in certain uses (preparing of white liquors, impurities removal of saturated salt solution, etc.) [25]. The reaction of CO₂ with sodium hydroxide (NaOH) to produce sodium carbonate (Na₂CO₃) is considered [26]:



NaOH offers fast absorption, producing a valuable product with commercial interest in 2015, sodium carbonate world production rounded 53.4 millions of tons [25]. NaOH can be taken from the waste streams coming from Mercox Towers [27] or from subproduct flows of chlor-alkali industry [28]. In this latter case, the use of NaOH-containing streams for CO₂ capture opens the opportunity to implement an integrated (membrane) process; i.e., CO₂ capture & sodium carbonate crystallization—for the valorization of the wastewater in an internal process loop on the chlor-alkali

industry. The interest of this approach is given because the brines (NaCl streams), used as raw material in the electro dialysis for the NaOH production, require a previous purification using Na_2CO_3 . Thus, NaOH-containing streams would reach both the CO_2 removal and the carbonate production, leading to a self-sufficient industry. Furthermore, the footprint associated to the electricity generation (electrodialysis is the larger energy-consuming step) would be minimized.

The main objective of this manuscript is to compare the performance of the membrane based-absorption with the conventional absorption system using NaOH aqueous solutions as the absorption solvent. The different species involved in the absorption process are monitored and the influence of the main parameters (concentration and flow rates of both gas and liquid phases) on the mass transfer are addressed.

2. Experimental

2.1. Chemicals

The feed stream is a mixture of air (piston compressor entrained by an electric motor and delivering a maximum pressure of 8 bars) and CO_2 (industrial carbon dioxide at 20 bars, Praxair). The absorption solution was made by dissolving NaOH pellets (sodium hydroxide, NaOH solid, AnalaR Normapur 98.5%) in deionized water (electrical resistivity of 18.2 $\text{M}\Omega/\text{cm}$).

2.2. Experimental Set up and Operation

The CO_2 capture by NaOH solution was experimentally studied by means of a membrane contactor and an absorption column connected in parallel so that both set ups can be used independently in the same installation (Figure 1).

The absorption column was a packed column UOP7-MKII Gas Absorption Column, Armfield Ltd. (Ringwood, UK). The membrane contactor was the 2.5 × 8 Extra-Flow Module™ Liqui-Cel®, Membrana GmbH (Wuppertal, Germany). Characteristics of both devices are collected in Table 1.

Table 1. Characteristics of the packed column and the hollow fiber contactor.

Packed Column		Hollow Fiber Membrane Contactor	
Parameters	Data from manufacturer	Parameters	Data from manufacturer
Walls material	Acrylic	Membrane/Potting Material	Polypropylene/Polyethylene
Column diameter (m)	0.8	Fiber i.d./o.d (μm)	240/300
Column packing	Raschig rings	Wall thickness (μm)	40
Raschig rings dimensions (mm × mm)	10 × 10	Effective pore size (μm)	0.04
Raschig rings material	Glass	Porosity (%)	40
Column length (m)	1.4	Effective fiber length (m)	0.16
Raschig rings specific area (m^2/m^3)	440	Effective membrane surface area (m^2)	1.4
Packing volume (L)	7	Number of fibers	10,200

In both systems a flue gas (mixture air- CO_2) was contacted with an absorbent (NaOH) in counter-current mode. The composition of the gas and liquid phases were measured at the inlet and the outlet of the absorbers: CO_2 concentration in the gas was directly measured by sensors and plotted on the console screen. Physical and chemical absorptions took place and, therefore, new components appeared (carbonates and bicarbonates). The concentration of the hydroxides, carbonates and bicarbonates was measured at the inlet of the absorbers; i.e., whose values correspond to the composition of the feed tank—and at the outlet; i.e., after the absorption takes places. The inlet

and outlet samples were taken at the same time every 20 min. The ion concentrations in the aqueous solution were indirectly calculated by titrations of the liquid samples (see Section 2.3). The gas coming out from the column/contactor; i.e., air and CO₂ not absorbed—is released to the atmosphere while the liquid phase works in a closed loop, returning to the sump tank during the 80 min of each experiment.

In the case of the column, the absorbent was pumped to the top of the packed column (filled with glass Raschig rings, with an interfacial area of 3.1 m²) and fell through it by gravity. At the bottom, the gas stream is introduced. The CO₂ from the gas diffuses to the liquid phase and is chemically absorbed by NaOH in the liquid film surrounding the packing material. The column has an interfacial area and a volume of 3.1 m² and 0.7 m³, respectively.

Regarding the membrane contactor, the fluid-fluid contact was produced in the pores of the more than ten thousand hollow fibers (the effective interfacial area is 1.4 m²). Gas circulated inside the fibers (lumen side) and the liquid run around the fibers (shell side). The module (including the housing) occupies 0.13 m³.

The pressure drop caused by the liquid phase was evaluated when varying the liquid and gas flow rates in the column from 1 to 7 L min⁻¹ and from 40 to 180 L min⁻¹, respectively. Liquid and gas flow rates ranged in the membrane contactor from 1 to 3 L min⁻¹ and from 10 to 24 L min⁻¹, respectively. The values of the pressure drop in both systems are addressed in the Appendix A as supporting information.

The presence of species in the system and the mass transfer coefficients were also analyzed for both the gas and the liquid streams. This study was carried out by varying the concentrations of the absorbent and the flue gas from 0.2 to 1 mol L⁻¹ of NaOH and from 10 to 15% of CO₂, respectively. The effect of the liquid and gas flow rates was also studied, as previously mentioned, for the pressure drop study.

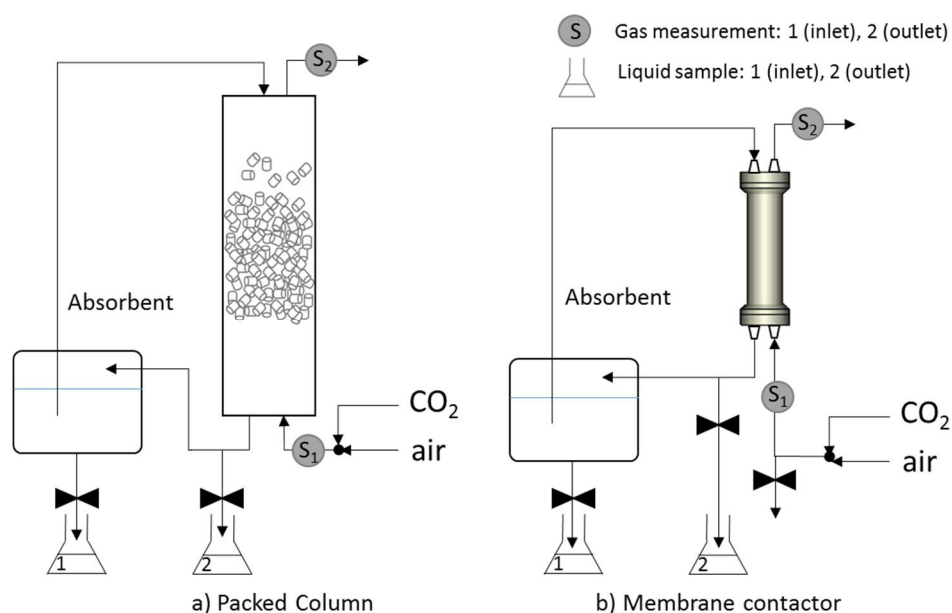


Figure 1. Experimental set ups for CO₂ capture.

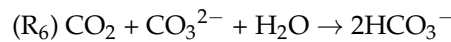
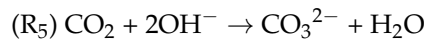
2.3. Analytical Methods

The composition of both gas and liquid was analyzed in order to evaluate the variation of present species in the system.

The CO₂ concentration in the gas phase at the inlet and outlet of both the column and the membrane contactor was measured by a AWM5000 Series Microbridge Mass Airflow Sensor. It operates

on the theory that air flow directed across the surface of a sensing element causes heat transfer and output voltage varies in proportion to the mass of air.

Focused on the liquid phase, the titration method was employed to determine the concentration of the species; i.e., OH^- , CO_3^{2-} and HCO_3^- . During the experimental work, the absorption of CO_2 led to carbonates in the solution until all the NaOH was exhausted at the moment when the bicarbonates are produced, as it is described in reactions R_5 and R_6 . The samples were treated with HCl and two color indicators; i.e., phenolphthalein and methyl orange.



On one hand, when NaOH is still present in the solution (R_5), titration starts with the hydroxide reacting with a volume V_1 of HCl (R_7). This volume indicates that all the OH^- was neutralized and only bicarbonate is present in the solution, which corresponds to the moment that the sample becomes colorless from the initial purple given by the phenolphthalein. Subsequently, a two-step reaction occurs, consuming two moles of HCl to neutralize one mole of carbonate (R_8 and R_9). Here, a volume V_2 of HCl is used to neutralize all the bicarbonates—titration finishes when the yellow color of the solution given by the methyl orange becomes totally pink. On the other hand, when no more NaOH is present in the sample, the absorption takes place according to R_6 . Then, titration consumes a volume V_1 of HCl to convert all the carbonates into bicarbonates (R_8) and a volume V_2 of HCl to finally produce H_2CO_3 . The calculations of the volumes and species concentrations are summarized in Table 2.

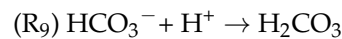
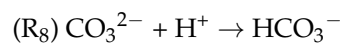
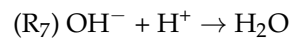


Table 2. Volumes and species concentrations obtained by titration.

	Volumes	Species Concentration
NaOH still in solution	$V_{total} = V_1 + V_2$ $V_{\text{CO}_3^{2-}} = 2 \cdot V_2$ $V_{\text{OH}^-} = V_{total} - V_{\text{CO}_3^{2-}}$	$[\text{OH}^-] = \frac{[\text{HCl}] \cdot V_{\text{OH}^-}}{V_{sample}}$ $[\text{CO}_3^{2-}] = \frac{[\text{HCl}] \cdot V_{\text{CO}_3^{2-}}}{V_{sample}}$
NaOH already exhausted	$V_{\text{CO}_3^{2-}} = 2 \cdot V_1$ $V_{\text{HCO}_3^-} = V_2 - V_1$	$[\text{CO}_3^{2-}] = \frac{[\text{HCl}] \cdot V_{\text{CO}_3^{2-}}}{V_{sample}}$ $[\text{HCO}_3^-] = \frac{[\text{HCl}] \cdot V_{\text{HCO}_3^-}}{V_{sample}}$

2.4. Mass Transfer Equations

The absorption rate allows the calculation of the overall mass transfer coefficient for both the packed column and the membrane contactor system, using Equation (1) (adapted from [29]).

$$r_{\text{CO}_2} = F_{a,i} \cdot \frac{p_{atm}}{R \cdot T_i} \tag{1}$$

where F_a is the volumetric rate of absorption of CO_2 (L s^{-1}) given by Equations (2) and (3), p_{atm} is the atmosphere pressure, R is the gas constant, T is the temperature and the subscript i represents either the column or the contactor.

$$F_{a,column} = \frac{(C_{\text{CO}_2,I} - C_{\text{CO}_2,II}) \cdot (F_{air} + F_{\text{CO}_2})}{100 \cdot 60} \tag{2}$$

$$F_{a,membrane} = \frac{(C_{CO_2,I} \cdot G_I - C_{CO_2,II} \cdot G_{II})}{100 \cdot 60} \quad (3)$$

where $C_{CO_2,I}$, $C_{CO_2,II}$, F_{air} , F_{CO_2} are the concentrations (vol %) of CO_2 at the inlet (I) and the outlet (II), and the flow rates of air and CO_2 of the packed column, respectively; and G_I and G_{II} are the inlet and outlet total flow gas of the membrane contactor, respectively.

Absorption rates were further used to calculate the overall mass transfer coefficient (K_{ov} , $\text{mol atm}^{-1} \text{m}^{-2} \text{s}^{-1}$) by means of the following equations for both, the packed column system – $K_{ov,c}$, Equation (4)– and the membrane contactor set up – $K_{ov,m}$, Equation (5), (adapted from [30]):

$$K_{ov,c} = \frac{r_{CO_2}}{a \cdot A \cdot H \cdot \Delta P_{lm,i}} \quad (4)$$

$$K_{ov,m} = \frac{r_{CO_2}}{a_{eff} \cdot \Delta P_{lm,i}} \quad (5)$$

where a is the specific area of packing per unit volume of the column ($\text{m}^2 \text{m}^{-3}$), A is the cross-sectional area of the tower (m^2), H is the packing height (m), ΔP_{lm} is the logarithmic mean driving force (see Appendix A) and a_{eff} is the effective gas-liquid contact area (m^2).

Finally, the efficiency removal of CO_2 (E , %) was measured according to the following equation [31]:

$$E(\%) = \frac{CO_{2,I} - CO_{2,II}}{CO_{2,I}} \cdot 100 \quad (6)$$

3. Results and Discussion

3.1. Variation of Species

Figure 2 represents the evolution of the ion concentrations over the time when the packed column is operated. Two trends describe the hydroxide, carbonate, and bicarbonate ion concentrations before (Figure 2a) and after (Figure 2b) the gas-liquid contact inside the column.

According to reaction R_5 , the depletion of NaOH and the production of the carbonates take place. Regarding the consumption of the NaOH, a first look allows us to conclude that the instantaneous reaction between the CO_2 and the hydroxide occurs as soon as both phases are in contact and when pH is still higher than 10. The drastic differences between the inlet and outlet concentration in the first 20 min corroborates the high selectivity of the absorbent to the contaminant. This rapid exhaustion of the initial absorbent will strongly influence the mass transfer coefficient in later calculations. In parallel, the presence of the carbonate ions increases over time as a consequence of the reaction. From 20 to 60 min, NaOH is still present in the sum tank but is not any more at the outlet of the column because all the NaOH contacting the CO_2 is reacting and the alkaline solution is close to the saturation in terms of absorption. In this time frame, carbonate concentration remains almost constant (around 0.1 M, the maximum to be produced according to the stoichiometry 2:1) at the outlet of the column because carbonates are still producing but also being consumed by the reaction with the CO_2 (R_6). Both reactions take place at the same time when the hydroxide concentration is quite low ($10 < \text{pH} < 8$). The total depletion of the 0.2 M of NaOH arrives in the following moments after 60 min of the process (Figure 2b) has passed, due to the fact that no more hydroxides are available at the outlet at this time and, since that moment, the profile corresponding to the inlet carbonate concentration, which was all the time below the outlet trend, is above up to the end of the process at 80 min. This can be explained because once the NaOH has totally disappeared ($\text{pH} < 8$), carbonates are the only species reacting with CO_2 producing bicarbonates. This second reaction is seen where both bicarbonate profiles remain in zero for 40 min but slowly increase, first appearing at the outlet of the column (Figure 2b) and, finally, when the presence of bicarbonate is high enough to be detected by titration in the feed tank (Figure 2a). At the end of the experiment, only carbonates and bicarbonates were in the solvent reservoir.

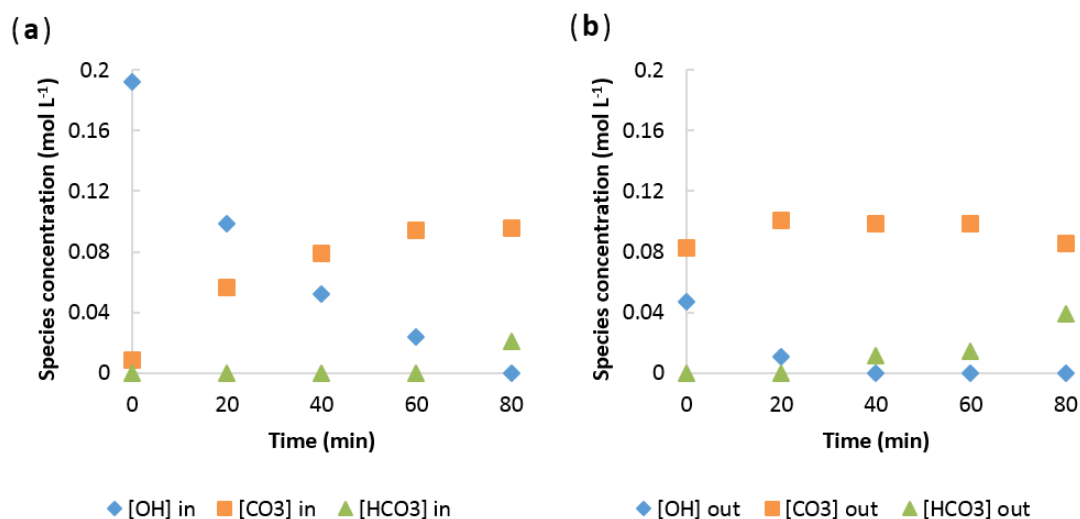


Figure 2. Evolution of inlet (a) and outlet (b) species concentration as a function of time in the packed column. CO₂ and NaOH initial concentrations are 10% and 0.2 mol L⁻¹, respectively; gas and liquid flow rates are 33 and 1 L min⁻¹; respectively.

Species concentrations collected in the column followed the same trend when the membrane contactor set up was evaluated. Figure 3 shows the evolution of hydroxides, carbonates and bicarbonates at the inlet and the outlet of the hollow fibers. Similar operating conditions were applied, except in the gas flow rate, being in this case 6.5 L min⁻¹ (33 L min⁻¹ in the packed column) due to the smaller dimension of the contactor. Inlet (Figure 3a) and outlet (Figure 3b) concentrations describe linear trends against the drastic absorption that occurs in the column. Here, NaOH depletion is slower due to the fact that less flue gas is coming into the contactor and, therefore, less amount of CO₂ reacts. Thus, the concentration of hydroxide remains higher (because the same initial volume was used in the sum tank) but the production of carbonate is also lower (stoichiometry is respected). Figure 3 shows that no bicarbonates appeared during the experiments because the NaOH concentration was high enough to absorb the CO₂ following the R₅ reaction, which did not allow the reaction with the carbonates (R₆). Thus, the reservoir only contained sodium hydroxide and carbonates at the end of the experiment.

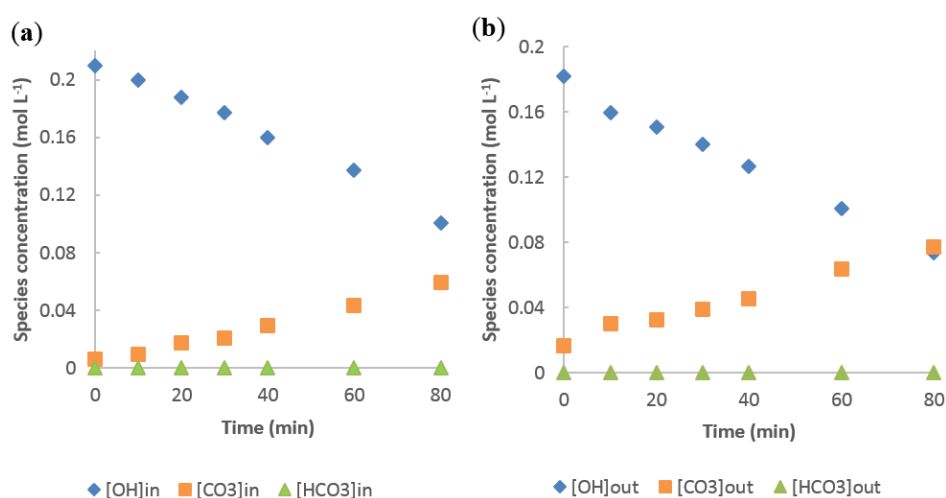


Figure 3. Evolution of inlet (a) and outlet (b) species concentration as a function of time in the membrane contactor. CO₂ and NaOH initial concentrations are 10% and 0.2 mol L⁻¹, respectively; gas and liquid flow rates are 6.5 and 1 L min⁻¹; respectively.

In summary, both technologies respond to the same physical and chemical mechanisms. Alkaline solutions, either if they are pure solutions (NaOH or Na₂CO₃) or mixtures NaOH/Na₂CO₃, can be used to capture the CO₂ and to finally produce the compound that is required. This approach could be extended to other alkaline solutions such as potassium hydroxide (KOH), leading to potassium carbonate (K₂CO₃) and/or bicarbonate (KHCO₃), which are largely used as cleaning and emulsifying agents [25], among other applications.

3.2. Mass Transfer Coefficient

The influence of four main variables; i.e., concentrations and flow rates of both flue gas and absorbent on the mass transfer carried out in both the packed column and the membrane—was studied according to the experimental conditions defined in Section 2.2 and the characterization methods in Section 2.3. Results are shown in the next sections.

3.2.1. Influence of the Flow Rates of the Fluids on the Mass Transfer Coefficient

The evolution of the species concentration aforementioned is characteristic of systems that work in batch mode. Nevertheless, power generation and CO₂ emissions are rarely interrupted, so refreshed solvents must be used to keep the concentration constant and, consequently, the same level of absorption. The way to simulate this scenario from the batch laboratory results is by calculating the mass transfer coefficients at the beginning of the experiment (time 20 min in this case) to ensure high concentration of NaOH and an almost constant concentration of CO₂ at the outlet gas. These results are addressed in Figures 4 and 5. Furthermore, the mass transfer coefficient for different concentrations of the NaOH and NaOH/Na₂CO₃ mixtures obtained in the laboratory are collected in Figure 6.

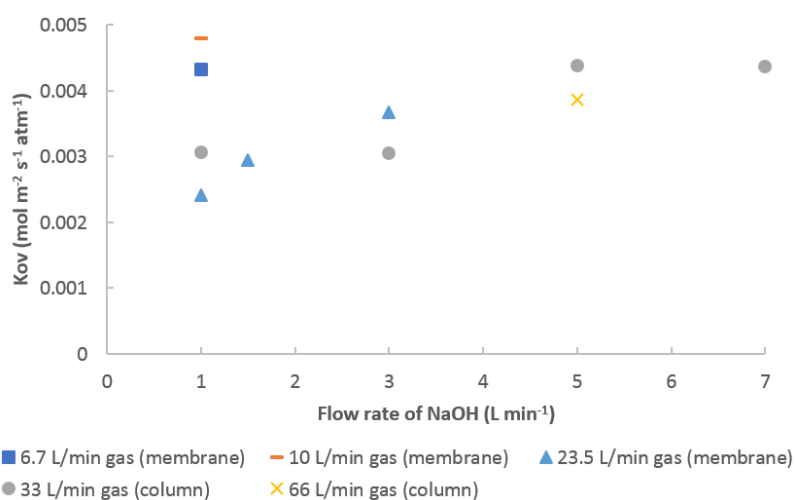


Figure 4. Mass transfer coefficient in function of the NaOH flow rate for different flue gas flow rates in the two set ups. The CO₂ and NaOH initial concentrations are 10% and 0.2 mol L⁻¹, respectively, for all the cases except the experimental point corresponding to 23.7 L min⁻¹ gas (membrane) and 3 L min⁻¹ of NaOH flowrate, where it was used as 15% of CO₂.

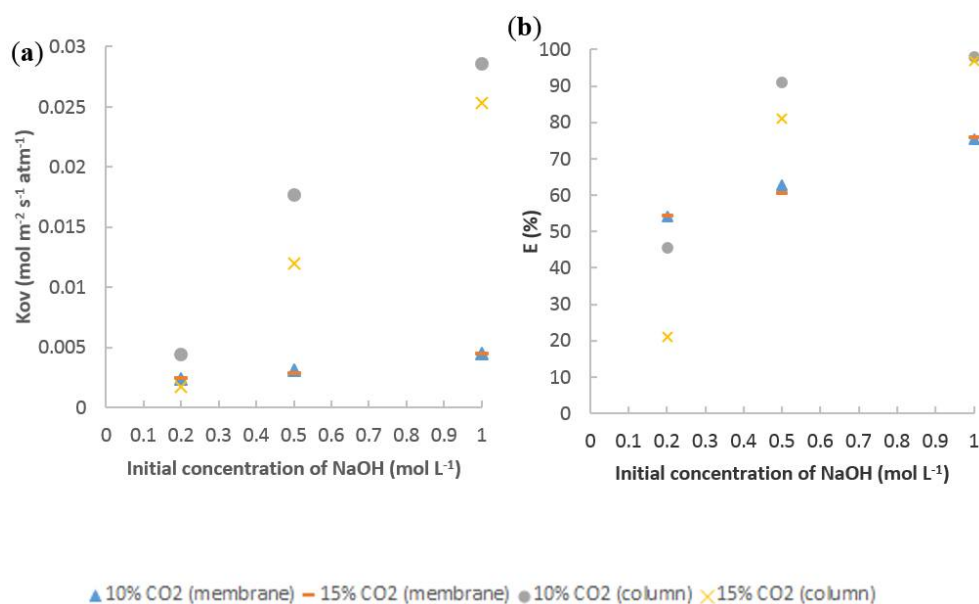


Figure 5. (a) Mass transfer coefficient in function of the NaOH initial concentration in the solvent for different CO₂ concentrations in the flue gas in the two set ups; (b) CO₂ removal efficiency. The solvent and the flue gas flow rates in the column and the membrane contactor are 5 and 33 L min⁻¹ and 1 and 23.5 L min⁻¹, respectively.

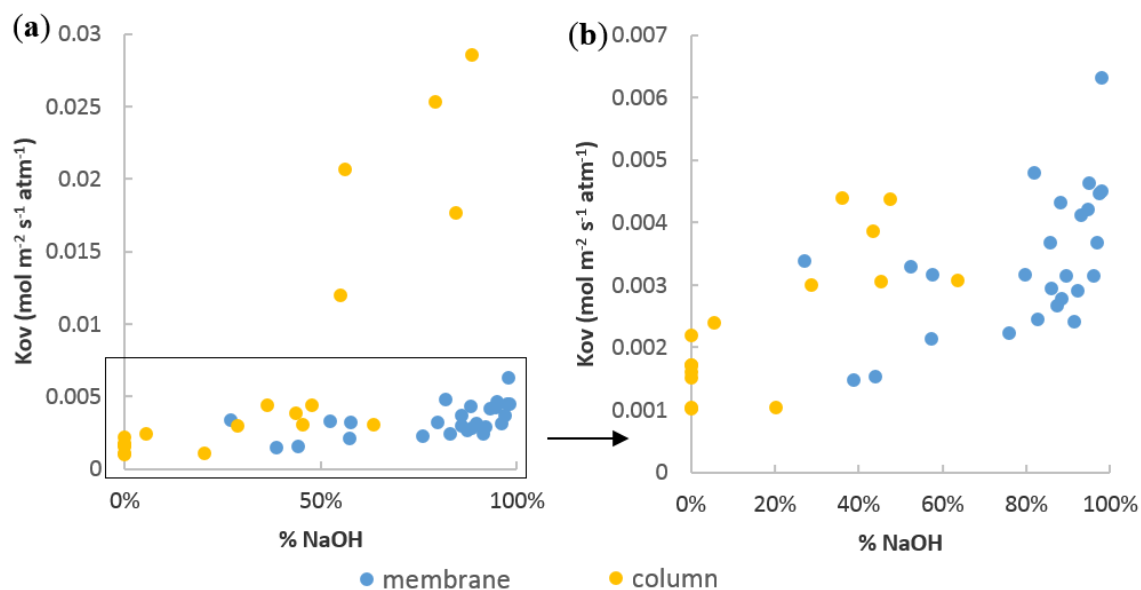


Figure 6. (a) Mass transfer coefficient in function of the %NaOH in the liquid solution in the two set ups; (b) Zoom of the bottom part of Figure 6a.

In Figure 4, mass transfer coefficients obtained by running both a packed column and the membrane contactor are plotted as a function of the solvent flow rates for different feed gas streams. In the column, the higher the solvent flow rate and the lower the flue gas velocity, the higher the mass transfer coefficient. For the studied operation conditions, when the liquid flow rate is increased from 1 to 7 L min⁻¹ in the column, the overall mass transfer coefficient increases by 42%. When the liquid stream is increased from 1 to 3 L min⁻¹ in the contactor, the overall mass transfer coefficient enhances by 51%. The higher the liquid flow rate, the more rapidly fresh NaOH enters the column/contactor, ensuring that CO₂ is efficiently absorbed. Furthermore, the turbulence that is generated decreases the

resistance in the liquid phase and, therefore, a better mixing of the phases within the absorber [32]. In the contactor, the membrane means an extra resistance, which is counterbalanced by reducing the liquid boundary layer by increasing the solvent flow rate. On the other hand, when the flue gas increases in the column from 33 L min^{-1} to the double, the overall mass transfer coefficient decreases by 12%. By increasing the increment of the flue gas from 10 to 23.5 L min^{-1} in the membrane contactor, this reduces the overall mass transfer coefficient around by 50%. While this parameter does not have a relevant effect on the column, it seems more shocking on the contactor. It is normally expected that the higher the gas flow rate, the lower the mass transfer resistance (inversely proportional to the mass transfer coefficient), as it occurs when the flue gas rises from 6.7 to 10 L min^{-1} . Nevertheless, the mass transfer coefficient is lower for a gas stream of 23.5 L min^{-1} . In this case, it was experimentally observed that bubbles appeared in the liquid phase; i.e., the other side of the membrane. This means that gas pressure overcomes the liquid one and, therefore, the gas-liquid contact was not only produced in the pores of the membrane but also in the liquid side. In other words, the gas pressure limitation of the membrane contactor was exceeded. Consequently, the mass transfer occurred but the efficiency decreased because the operating limitations were not respected. Therefore, this result is discussed with special caution.

The effect of the fluids also revealed that all the mass transfer coefficients addressed in Figure 4 share the same order of magnitude, although the exchange area in the membrane contactor is two times lower than in the column and the volume is also smaller. This verifies the idea that much lower mass transfer coefficients would be expected in the packed column at identical experimental conditions in both kind of absorbers (for example, liquid and gas streams of 1 L min^{-1} and 6.5 L min^{-1} , respectively), and, therefore, the process intensification would be directly identified. Nevertheless, it is needed to go further and to analyze the influence of the composition of the fluids, also in the efficiency on the elimination of the contaminant.

3.2.2. Influence of the Gas and Liquid Composition on the Mass Transfer Coefficient

Regarding the composition of the flue gas and the absorbent, Figure 5a displays the mass transfer coefficient calculated in both set ups when the NaOH initial concentration ranges from 0.2 to 1 mol L^{-1} and 10–15% CO_2 in the flue gas is used. Here, the overall mass transfer coefficient for 0.5 and 1 mol L^{-1} of NaOH is one order of magnitude higher than that obtained for 0.2 mol L^{-1} (also plotted in Figure 4). Thus, the effect caused by the variation of the flow rate shown in the previous section is negligible compared to the important effect of the NaOH concentration. High NaOH concentration increases the overall mass transfer coefficient due to the larger availability of hydroxide groups to react with CO_2 , which increases the absorption capacity of the solvent [33]. Regarding the flue gas composition, no effect is observed in the membrane contactor but it is noticeable in the column. In Figure 5a, both column profiles followed a parallel trend. Mass transfer coefficients are higher when the amount of CO_2 is lower in the flue gas. Again, more hydroxides remain in the feed tank because less reactions took place with the contaminant and, therefore, more OH^- ions are able to chemically absorb with CO_2 while passing through the packing, ensuring a high value of the coefficient. Similar mass transfer coefficients were obtained in both configurations when the concentration of the solvent was 0.2 M. Here, it should be remembered that the mass transfer in the column involves only the resistances of the gas and liquid boundaries but, in the membrane, a third extra resistance is present: the physical barrier [34]. In this case, the third resistance of the membrane does not mean a strong disadvantage compared with the absorption column. This specific scenario shows a hypothetical competition in terms of mass transfer but the CO_2 removal efficiency, plotted in Figure 5b, displays better results in the case of the conventional equipment, especially when 15% of CO_2 is treated. On the other hand, in the experiments with 0.5 and 1 mol L^{-1} of NaOH, the mass transfer coefficient values revealed an important difference between the packed column and the membrane contactor. It can be concluded that the most important variable affecting the mass transfer is the concentration of the solvent.

Figure 5b presents the CO₂ removal efficiency for the same group of experiments. Upslope trends obtained agree with the mass transfer coefficient profiles. The highest efficiencies were found in the column, where 97% of the CO₂ was eliminated when 1 mol L⁻¹ of initial NaOH was used for capturing both 10% and 15% of the CO₂ in the flue gas (75% elimination with the membrane) and more than 80% removal was reached with 0.5 mol L⁻¹. The lowest removal was obtained with the column when the concentration of the solvent was 0.2 mol L⁻¹, while the removal efficiency in the membrane contactor overcame the 50% for the same case. In summary, good removal efficiencies were obtained, similar to the literature previously reported [31], which may satisfy industrial requirements. Furthermore, it can be concluded that the concentration of NaOH is the most responsible parameter in absorption.

The mass transfer coefficients and the removal efficiency showed in Figures 4 and 5 must be considered conservative because they were calculated at time = 20 min, in which the initial concentration of NaOH had already decreased. Indeed, a removal efficiency of up to 97% was also obtained in the membrane contactor when the value at time 0 was used; i.e., few seconds after starting the experiment. In order to show a more realistic overview of results, according to the real sorbent concentration, Figure 6 displays the mass transfer coefficient of all the experiments made in the function of the percentage of the NaOH still present in the solution.

Five points in the upper part of Figure 6a highlight the rest of the experimental cases. These values correspond to the experiments where the initial NaOH concentration was 0.5 and 1 mol L⁻¹ in the column. A high initial concentration avoids the rapid exhaustion of the hydroxides, reaching best mass transfer and capturing more CO₂. These coefficients were obtained only when the first reaction between the contaminant and the hydroxides was involved. A barrier rounding the 50% NaOH/Na₂CO₃ limits the possibility to reach mass transfer coefficients one order of magnitude higher than the majority collected. Thus, as soon as the carbonate ions were more and more present, the coefficient became lower. This performance is more pronounced in the column but it can be also appreciated when the plot is zoomed, as it is addressed in Figure 6b. Here, when the NaOH has already disappeared, the smallest removal of CO₂ is reached because now the carbonates are the only species with the capacity to absorb; therefore, bicarbonates appear.

From an industrial point of view, a low coefficient means poorer yield of the equipment; i.e., the column or the contactor. Nevertheless, the efficiency of the whole set up did not follow the same logic; i.e., the worst efficiency of the equipment was not always the worst performance of the complete system. This performance is seen on the membrane contactor if both the coefficients and the removal are contrasted in opposition with the apparently more coherent trend in the column, where high mass transfer and CO₂ elimination perfectly fit each other.

The comparison between the packed column and the membrane module must take into account the dimensions of each technology. Although the flue gas and the absorbent flow rates in the column were slightly higher than the one used through the membrane contactor, the intensification is clearly demonstrated since a membrane contactor whose volume is 0.13 m³ is able to obtain similar results than a packed column of 0.7 m³. Thus, the intensification factor; i.e., the ratio between the packed column volume and the membrane contactor volume—is 5.38. Studies about packed columns and membrane contactors [35,36] collected intensification factors between 1.5 and 11 using monoethanolamine, diethanolamine, triethanolamine or piperazine as absorbents. None of the previous research using NaOH as a sorbent has been found that uses the intensification factor parameter.

4. Conclusions

A gas stream containing 10–15 vol % CO₂ has been treated in both a packed column and a membrane contactor set up, leading to the capture of the contaminant by means of a sodium hydroxide solution in order to finally obtain a valuable product (sodium carbonate) to be reused in the industry. The influence of the main operating parameters; i.e., concentration and flow rates of both the gas and the liquid phase, on the species evolution, the overall mass transfer coefficient and the CO₂ removal efficiency—was evaluated.

Rapid exhaustion of the NaOH was found when the CO₂ was captured in the column, being faster when the sorbent concentration was smaller. When no more hydroxides exist, a secondary reaction between the carbonates and the contaminant produces bicarbonates. This becomes important because it opens the possibility to obtain different products and, therefore, further industrial applications will determine the components of interest. The evolution of the species in the membrane contactor followed the same trend.

The best and the worst mass transfer coefficients and CO₂ removal efficiencies were found in the column and intermediate values corresponding to the membrane contactor were set up. Thus, the column offered some mass transfer coefficients one order of magnitude higher than in the membrane contactor, corresponding to the experiments where 0.5 and 1 mol L⁻¹ of NaOH, but the major part of the results shared the same coefficient value range (0.001–0.0065). Again, the composition of the sorbent implies the stronger effect on the characterization parameters. Moreover, when no more NaOH were in the process, the contaminant elimination decayed until 21%, far from the 97% reached with the highest hydroxide content.

Regarding the flow rates of the fluids, the higher the absorbent velocity and the lower the gas fluent, the better the mass transfer. Nevertheless, the influence of this parameter may be negligible in comparison to the strength of the NaOH concentration effect.

Results allow us to conclude that, firstly, the technical viability to capture CO₂ with the novelty offered by the membrane technology is a fact and, secondly, that it will become a powerfully competitive alternative to traditional absorption, including an intensification factor of 5.38.

Author Contributions: I.R.S. and P.L. conceptualized this research work; N.C. carried out the investigation tasks and prepared the original draft. I.R.S. and P.L. wrote, reviewed and edited the manuscript. P.L. supervised the investigation and acquired the funding.

Acknowledgments: I. Ruiz Salmón would like to acknowledge the support of the research group Ecoefficient Processes for Sustainable Industrial Chemical and Biochemical Engineering in the department of Materials and process engineering (IMAP) of the Institute of Mechanics, Materials and Civil Engineering (iMMC), at the Université catholique de Louvain. The authors acknowledge the financial support by the Fonds spéciaux de recherche (FSR) of the Université catholique de Louvain.

Conflicts of Interest: The authors declare no conflict of interest.

Appendix A

Logarithmic mean driving forces are given by the following equations:

$$\Delta P_{lm,column} = \frac{y_{inlet} - y_{outlet}}{\ln\left(\frac{y_{inlet}}{y_{outlet}}\right)} \cdot \frac{p_{atm}}{100} \quad (A1)$$

$$\Delta P_{lm,contactor} = \frac{y_{inlet} - y_{outlet}}{\ln\left(\frac{y_{inlet}}{y_{outlet}}\right)} \cdot p_{mean} \quad (A2)$$

where, y_{inlet} and y_{outlet} are the inlet and outlet partial pressures (%) and p_{mean} is the average pressure in the lumen side (atm) in the membrane contactor.

Pressure Drop Measurement

Pressure drop in the experimental set ups was measured due to the influence that flooding may have in the CO₂ absorption and, therefore, the mass transfer. Figure A1 represents the variation of the pressure drop according to the air and liquid flow rates in the packed column. Two observations require attention. First, the higher the air/liquid flow rate, the higher the pressure drop. For a fixed gas flow rate value, it is observed that the distance between two consecutive points becomes larger when the liquid flow rate increases. Here, the pressure drop increment is due to the resistance offered by the liquid falling against the air flowing up. Meanwhile, liquid flow rates follow a linear trend, with an almost constant distance between consecutive points and a slow change in the slope. This is

due to the liquid holdup and an additional resistance to the air flow. The stronger effect on the pressure drop comes, then, from the liquid flow and it can be seen with an easy example from the graph: a pressure drop of 10 mbar could be measured with an air/liquid flow of 170/1 L min⁻¹ but also with 50/5 L min⁻¹.

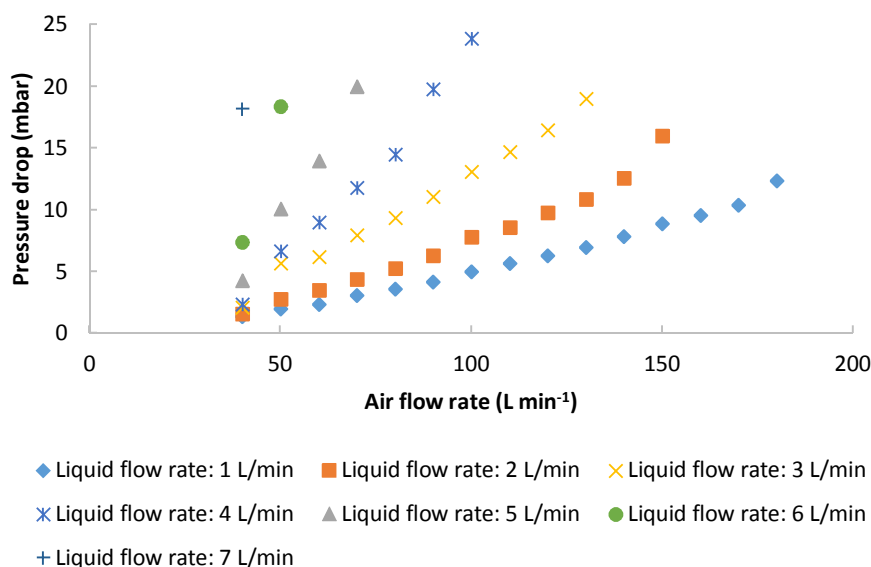


Figure A1. Pressure drop as a function of the air flow rate for different liquid flow rates.

Secondly, the pressure drop for the range studied does not mean relevant importance. The maximum air flow rate in the CO₂ capture experiments was 66 L min⁻¹, where the highest pressure drop found for this is 20 mbar, which corresponds to a liquid flow of 5 L min⁻¹. Even in the larger pressure drop value collected (24 mbar from air/liquid streams of 100/4 L min⁻¹) is very far from atmospheric pressure (1013 mbar). Thus, the pressure drop was considered negligible in other calculations; i.e., volumetric rate of absorption of CO₂ and the mass transfer coefficient.

Regarding the membrane contactor system, the flow capacity for both gas and liquid was lower than the column. The pressure drop was here evaluated in two different configurations based on the Figure 1b. A valve was placed before the inlet of the lumen side to ensure that the CO₂ sensor was not flooded by an excessive gas flow. This may suppose an unreliable CO₂ concentration measurement. The influence of the opened/closed valve in the pressure drop along the membrane contactor was then evaluated and plotted in Figure A2. It shows the evolution of the pressure drop for both configurations when the gas flow is increased. Differences are evident and a closed valve system shows pressure drops more than four times greater than the opened valve configuration for the range analyzed. This is the case of a gas flow of 20 L min, where the pressure drop is 100 and 24 mbar for the closed valve and the opened valve settings, respectively. These differences are clearly due to the release of gas by the opened valve finding the easiest way to escape but also because of the narrowing from the pipes connected to the contactor (less than 10 mm) to the hollow fibers (10,200 fibers with an internal diameter of 240 μm). Although the flue gas fed to the rest of the experiments did not exceed 10 L min⁻¹, the pressure drop already represents 40 mbar, which is the double of the maximum value obtained for the worst case in the packed column. As occurred with calculations about the packed column, the pressure drop is negligible with regards to the atmospheric pressure. Nevertheless, the opened valve configuration may affect the species evolution and, therefore, the mass transfer coefficient. Thus the result so results require careful consideration.

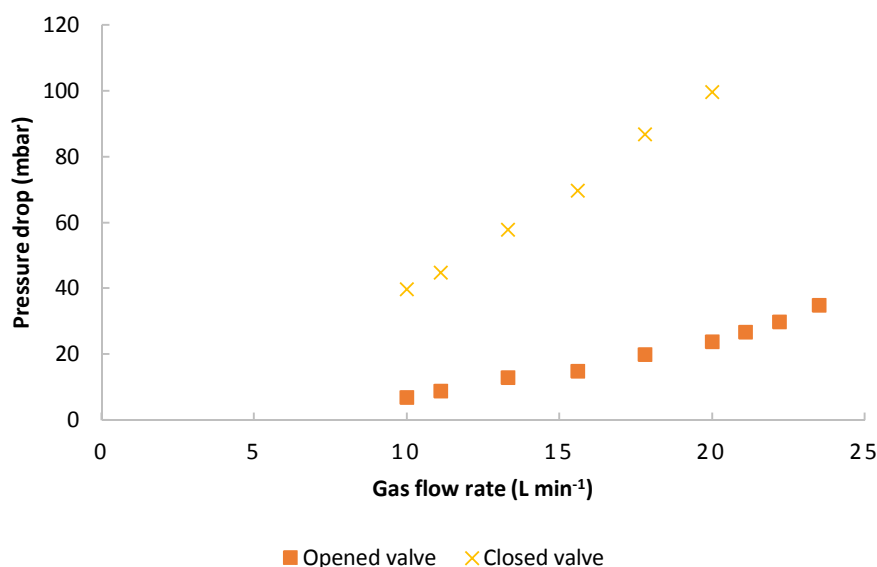


Figure A2. Pressure drop as a function of the gas flow rate for two configurations.

References

- Houghton, J.T.; Ding, Y.D.J.G.; Griggs, D.J.; Noguera, M.; van der Linden, P.J.; Dai, X.; Maskell, K.; Johnson, C.A. *Climate Change 2001: The Scientific Basis*; The Press Syndicate of the University of Cambridge: Cambridge, UK, 2001.
- NASA Jet Propulsion Laboratory. Available online: <http://climate.nasa.gov> (accessed on 11 February 2018).
- Kuramochi, T.; Ramírez, A.; Turkenburg, W.; Faaij, A. Comparative assessment of CO₂ capture technologies for carbon-intensive industrial processes. *Prog. Energy Combust. Sci.* **2012**, *38*, 87–112. [[CrossRef](#)]
- Rao, A.B.; Rubin, E.S. A technical, economic, and environmental assessment of amine-based CO₂ capture technology for power plant greenhouse gas control. *Environ. Sci. Technol.* **2002**, *36*, 4467–4475. [[CrossRef](#)] [[PubMed](#)]
- Favre, E. Membrane processes and postcombustion carbon dioxide capture: Challenges and prospects. *Chem. Eng. J.* **2011**, *171*, 782–793. [[CrossRef](#)]
- Gabelman, A.; Hwang, S.T. Hollow fiber membrane contactors. *J. Memb. Sci.* **1999**, *159*, 61–106. [[CrossRef](#)]
- Luis, P.; Van der Bruggen, B. The role of membranes in post-combustion CO₂ capture. *Greenh. Gas Sci. Technol.* **2013**, *3*, 318–337. [[CrossRef](#)]
- Ramdin, M.; de Loos, T.W.; Vlugt, T.J. State-of-the-art of CO₂ capture with ionic liquids. *Ind. Eng. Chem. Res.* **2012**, *51*, 8149–8177. [[CrossRef](#)]
- Luis, P.; Ortiz, I.; Aldaco, R.; Irabien, A. A novel group contribution method in the development of a QSAR for predicting the toxicity (Vibrio fischeri EC 50) of ionic liquids. *Ecotoxicol. Environ. Saf.* **2007**, *67*, 423–429. [[CrossRef](#)] [[PubMed](#)]
- Anthony, E.J. Ca looping technology: current status, developments and future directions. *Greenh. Gas Sci. Technol.* **2011**, *1*, 36–47. [[CrossRef](#)]
- Romeo, L.M.; Catalina, D.; Lisbona, P.; Lara, Y.; Martínez, A. Reduction of greenhouse gas emissions by integration of cement plants, power plants, and CO₂ capture systems. *Greenh. Gas Sci. Technol.* **2011**, *1*, 72–82. [[CrossRef](#)]
- Wang, Q.; Luo, J.; Zhong, Z.; Borgna, A. CO₂ capture by solid adsorbents and their applications: current status and new trends. *Energy Environ. Sci.* **2011**, *4*, 42–55. [[CrossRef](#)]
- Samanta, A.; Zhao, A.; Shimizu, G.K.; Sarkar, P.; Gupta, R. Post-combustion CO₂ capture using solid sorbents: A review. *Ind. Eng. Chem. Res.* **2011**, *51*, 1438–1463. [[CrossRef](#)]
- Liu, J.; Thallapally, P.K.; McGrail, B.P.; Brown, D.R.; Liu, J. Progress in adsorption-based CO₂ capture by metal-organic frameworks. *Chem. Soc. Rev.* **2012**, *41*, 2308–2322. [[CrossRef](#)] [[PubMed](#)]

15. Luis, P.; Van Gerven, T.; Van der Bruggen, B. Recent developments in membrane-based technologies for CO₂ capture. *Prog. Energy Combust.* **2012**, *38*, 419–448. [[CrossRef](#)]
16. Close, J.J.; Farmer, K.; Moganty, S.S.; Baltus, R.E. CO₂/N₂ separations using nanoporous alumina-supported ionic liquid membranes: Effect of the support on separation performance. *J. Memb. Sci.* **2012**, *390*, 201–210. [[CrossRef](#)]
17. Roberson, L.M. The upper bound revisited. *J. Memb. Sci.* **2008**, *320*, 390–400. [[CrossRef](#)]
18. Li, B.; Duan, Y.; Luebke, D.; Morreale, B. Advances in CO₂ capture technology: A patent review. *Appl. Energy* **2013**, *102*, 1439–1447. [[CrossRef](#)]
19. Merkel, T.C.; Lin, H.; Wei, X.; Baker, R. Power plant post-combustion carbon dioxide capture: An opportunity for membranes. *J. Memb. Sci.* **2010**, *359*, 126–139. [[CrossRef](#)]
20. Feng, C.; Wang, R.; Zhang, H.; Shi, L. Diverse morphologies of PVDF hollow fiber membranes and their performance analysis as gas/liquid contactors. *J. Appl. Polym. Sci.* **2011**, *119*, 1259–1267. [[CrossRef](#)]
21. Luis, P.; Van Aubel, D.; Van der Bruggen, B. Technical viability and exergy analysis of membrane crystallization: Closing the loop of CO₂ sequestration. *Int. J. Greenh. Gas Control* **2013**, *12*, 450–459. [[CrossRef](#)]
22. Ye, W.; Luis Alconero, P.; Van der Bruggen, B. Carbon Dioxide Recovery by Membrane Assisted Crystallization. In Proceedings of the International Conference on Chemical Science and Engineering (ICCSSE 2013), Zurich, Switzerland, 30–31 July 2013.
23. Ye, W.; Wu, J.; Ye, F.; Zeng, H.; Tran, A.T.; Lin, J.; Luis, P.; Van der Bruggen, B. Potential of osmotic membrane crystallization using dense membranes for Na₂CO₃ production in a CO₂ capture scenario. *Cryst. Growth Des.* **2015**, *15*, 695–705. [[CrossRef](#)]
24. Ruiz Salmón, I.; Janssens, R.; Luis, P. Mass and heat transfer study in osmotic membrane distillation-crystallization for CO₂ valorization as sodium carbonate. *Sep. Purif. Technol.* **2017**, *176*, 173–183. [[CrossRef](#)]
25. US Geological Survey & Orienteering S (Ed.) *Mineral Commodity Summaries, 2017*; Government Printing Office: Washington, DC, USA, 2017.
26. Astarita, G. Absorption of carbon dioxide into alkaline solutions in packed towers. *Ind. Eng. Chem. Fund.* **1963**, *2*, 294–297. [[CrossRef](#)]
27. Keramati, N.; Moheb, A.; Ehsani, M.R. Effect of operating parameters on NaOH recovery from waste stream of Merox tower using membrane systems: Electrodialysis and electrodeionization processes. *Desalination* **2010**, *259*, 97–102. [[CrossRef](#)]
28. Moussallem, I.; Jörisen, J.; Kunz, U.; Pinnow, S.; Turek, T. Chlor-alkali electrolysis with oxygen depolarized cathodes: History, present status and future prospects. *J. Appl. Electrochem.* **2008**, *38*, 1177–1194. [[CrossRef](#)]
29. Mavroudi, M.; Kaldis, S.P.; Sakellaropoulos, G.P. A study of mass transfer resistance in membrane gas–liquid contacting processes. *J. Memb. Sci.* **2006**, *272*, 103–115. [[CrossRef](#)]
30. Li, J.L.; Chen, B.H. Review of CO₂ absorption using chemical solvents in hollow fiber membrane contactors. *Sep. Purif. Technol.* **2005**, *41*, 109–122. [[CrossRef](#)]
31. Lin, C.C.; Chen, B.C. Carbon dioxide absorption into NaOH solution in a cross-flow rotating packed bed. *J. Ind. Eng. Chem.* **2007**, *13*, 1083–1090.
32. Ndiritu, H.; Kibicho, K.; Gathitu, B.B. Influence of flow parameters on capture of carbon dioxide gas by a wet scrubber. *J. Power Technol.* **2013**, *93*, 9–15.
33. Zeng, Q.; Guo, Y.; Niu, Z.; Lin, W. The absorption rate of CO₂ by aqueous ammonia in a packed column. *Fuel Process. Technol.* **2013**, *108*, 76–81. [[CrossRef](#)]
34. Chabanon, E.; Bounaceur, R.; Castel, C.; Rode, S.; Roizard, D.; Favre, E. Pushing the limits of intensified CO₂ post-combustion capture by gas–liquid absorption through a membrane contactor. *Chem. Eng. Process.* **2015**, *91*, 7–22. [[CrossRef](#)]
35. Albarracin-Zaidiza, D.; Belaissaoui, B.; Roizard, D.; Favre, E.; Rode, S. Stripping of CO₂ in post-combustion capture with chemical solvents: Intensification potential of hollow fiber membrane contactors. *Energy Procedia* **2017**, *114*, 1334–1341. [[CrossRef](#)]
36. Favre, E.; Svendsen, H.F. Membrane contactors for intensified post-combustion carbon dioxide capture by gas–liquid absorption processes. *J. Memb. Sci.* **2012**, *407*, 1–7. [[CrossRef](#)]

